JOURNAL OF GEOPHYSICAL RESEARCH, VOL. 113, C02009, doi:10.1029/2007JC004338, 2008

Surface heat fluxes from the NCEP/NCAR and NCEP/DOE reanalyses at the Kuroshio Extension Observatory buoy site

Masahisa Kubota,[1] Noriyasu Iwabe,[1] Meghan F. Cronin,[2] and Hiroyuki Tomita[3]

Received 15 May 2007; revised 2 August 2007; accepted 20 August 2007; published 13 February 2008.

[1] Surface heat fluxes from the Kuroshio Extension Observatory (KEO) buoy are compared with surface heat fluxes from the National Centers for Environmental Prediction (NCEP)/National Center for Atmospheric Research reanalysis (NRA1) and NCEP/Department of Energy reanalysis (NRA2). KEO surface measurements include downward solar and longwave radiation, wind speed and direction, relative humidity, rain rate, and air and sea surface temperature. For solar radiation, NRA2 had better agreement with KEO than NRA1. Both reanalyses underestimated shortwave radiation in summer and slightly overestimated it in winter. Turbulent surface heat fluxes are estimated with the KEO surface data using the Coupled Ocean-Atmosphere Response Experiment (COARE) version 3.0 bulk algorithm. Both NRA1 and NRA2 latent heat flux (LHF) are larger than KEO LHF, consistent with previous studies. However, the comparison shows larger errors than previously thought. Indeed, the latent heat flux bias for NRA1 is 41 W m^{-2} and for NRA2 is 62 W m^{-2} (indicating that the bias between NRA1 and NRA2 is 21 W m^{-2}). For latent heat flux, the large bias is caused primarily by the NRA bulk flux algorithm, while the root mean square (RMS) error is caused primarily by errors in the NRA meteorological variables. The combination of the biases for each heat flux is such that total NRA heat transfer from the ocean to the atmosphere is considerably larger than observed by KEO. These results highlight the importance of maintaining in situ observations for monitoring surface heat fluxes in the Kuroshio/Kuroshio Extension regions.

Citation: Kubota, M., N. Iwabe, M. F. Cronin, and H. Tomita (2008), Surface heat fluxes from the NCEP/NCAR and NCEP/DOE reanalyses at the Kuroshio Extension Observatory buoy site, *J. Geophys. Res.*, *113*, C02009, doi:10.1029/2007JC004338.

1. Introduction

[2] By transporting heat energy from low latitudes to midlatitudes, western boundary currents such as Kuroshio and Gulf Stream play an important role in making the Earth's global climate mild. As huge heat energy is transported poleward and into the subtropical gyre, the heat energy is released from the ocean surface and actively warms the atmosphere. The extremely high air-sea fluxes in Kuroshio and Kuroshio Extension regions are some of the largest found in the entire basin. Although these air-sea fluxes are critical to the global climate system, monitoring the in situ air-sea interactions is extremely challenging owing to the strong ocean currents and winter winds. However, in June 2004, as a contribution to the global network of Ocean Sustained Interdisciplinary Time series Environment observation Systems (OceanSITES) time series reference sites, a surface buoy, referred to as the Kuroshio Extension Observatory (KEO), was deployed by the National Oceanic and Atmospheric Administration (NOAA) in the Kuroshio Extension recirculation gyre.

[3] Global ocean surface flux provided by reanalysis is widely used for various studies because of their long and consistent time series, and homogeneous spatial resolution. Popular reanalysis products include, for example, the 40-year European Centre for Medium-Range weather Forecasts (ECMWF) reanalysis (ERA40), the National Centers for Environmental Prediction-National Center for Atmospheric Research (NCEP-NCAR) reanalysis NRA1 [*Kalnay et al.*, 1996], and the NCEP-Department of Energy (DOE) reanalysis NRA2 [*Kanamitsu et al.*, 2000]. Global ocean surface flux data constructed from satellite data, such as the Japanese Ocean Flux data sets with Use of Remote sensing Observations (J-OFURO) [*Kubota et al.*, 2002] and Goddard Satellite-based Surface Turbulent Fluxes (GSSTF) [*Chou et al.*, 2003], are also becoming more widely used. To gain confidence in these products, quantitative comparisons against independent data sets within a variety of different regions are required.

[4] Surface buoys can provide long, continuous, high-quality air-sea flux time series and these data sets are being used increasingly to assess the gridded products [e.g., *Josey*, 2001; *Sun et al.*, 2003; *Jiang et al.*, 2005; *Cronin et al.*, 2006a, 2006b]. Comparison with research quality ship-based measurements [*Cronin et al.*, 2006a] as well as

[1] School of Marine Science and Technology, Tokai University, Shimizu, Japan.
[2] Pacific Marine Environmental Laboratory, NOAA, Seattle, Washington, USA.
[3] Institute of Observational Research for Global Change, Japan Agency for Marine and Earth Science Technology, Yokosuka, Japan.

0148-0227/08/2007JC004338$09.00

shore-based studies [*Payne et al.*, 2002] indicate that buoy turbulent heat fluxes have an accuracy of approximately 10 W m^{-2} and the radiative fluxes have a similar accuracy. Using Woods Hole Oceanographic Institution research buoy measurements made during the Subduction Experiment in the Northeast Atlantic, *Josey* [2001] assessed the accuracy of surface heat flux from ERA and NRA1. He reported that both reanalyses persistently underestimate the ocean heat gain in this region owing to a combination of underestimated shortwave gain and overestimated latent heat loss. Similar results were found by *Sun et al.* [2003] using a more extensive Atlantic buoy data set that included not only the Subduction Experiment buoys, but also the PIRATA buoys in the tropical Atlantic, and buoys in the western north Atlantic. As was found by *Moore and Renfrew* [2002], *Sun et al.* [2003] found that the systematic overestimation of the turbulent heat fluxes in the numerical weather prediction products (NWPs) depend upon the regions and upon the bulk flux algorithm. In particular, the NWP fluxes changed significantly when the TOGA COARE flux algorithm was used to recalculate the fluxes.

[5] In the North Pacific there are very few surface moorings. Using monthly-mean objective analysis data (University of Wisconsin–Milwaukee (UWM) Comprehensive Ocean-Atmosphere Data Set (COADS) [*da Silva et al.*, 1994]), *Moore and Renfrew* [2002] assessed NRA1 and ERA15 surface turbulent heat flux over the western boundary currents of the North Atlantic and North Pacific Oceans. They found NRA1 surface turbulent heat flux contain significant systematic errors in these regions, with somewhat poorer agreement in the Kuroshio region than in the Gulf Stream region. *Moore and Renfrew* [2002] pointed out that the errors are associated with shortcomings in the bulk flux algorithm employed and presented a more appropriate bulk flux algorithm. *Qiu et al.* [2004] analyzed decadal-long surface meteorological measurements from a Japan Meteorological Agency buoy at 29°N, 135°E to elucidate the surface air-sea flux forcing in the western North Pacific Ocean. They also carried out a comparison between the heat fluxes estimated using the buoy measurements and those from NRA1 and pointed out that the daily NRA1 product overestimates both the incoming solar radiation at sea surface and the turbulent heat flux amplitude associated with the individual weather events, although the NRA1 product captures the timing and relative strength of the synoptic-scale net heat flux forcing very well.

[6] In June 2004, the KEO buoy was deployed in the Kuroshio Extension recirculation gyre at 144.6°E, 32.4°N to monitor air-sea heat, moisture and momentum fluxes, and upper ocean temperature and salinity. In early November 2005, midway through the second deployment year, the KEO buoy broke away from its anchor and had to be recovered. The KEO was not redeployed again until May 2006. The purpose of this paper is to use data from the first deployment year of the KEO surface buoy to assess the NRA1 and NRA2 heat fluxes in the Kuroshio Extension recirculation gyre. Because the ERA-40 ends in August 2002 (before the KEO buoy was deployed), we cannot use the KEO data to assess ERA-40. Likewise, assessment of the J-OFURO product and other products will be postponed until these products are updated and have more overlap with the KEO time series. The assessment demonstrates the importance of the monitoring observation by the KEO buoy.

2. Data

[7] The KEO buoy is essentially an enhanced Tropical Atmosphere and Ocean (TAO) buoy [e.g., *McPhaden et al.*, 1998; *Cronin et al.*, 2006a] modified for the severe conditions of the Kuroshio Extension region. In particular, in order to measure and survive the strong winds in this region, wind velocity at 4 m height was measured with a Väisälä Ultrasonic WS425 during the first deployment (June 2004 to May 2005) and a Gill WindSonic anemometer during the second deployment (June 2005 to November 2005). According to manufacture specifications, the Väisälä wind sensor has 0.1 m s^{-1} resolution and an accuracy of ±0.135 m s^{-1} or 3%. The Gill wind sensor has a 0.01 m s^{-1} resolution and ±2% accuracy. Winds are sampled at 2-hz and averaged for 2 minutes every 10 minutes at 4-m altitude. All other sensors were similar to those described by *Cronin et al.* [2006a]. In particular, in addition to winds, the KEO buoy measured solar and longwave radiation at 2-minute intervals, rain rate at 1-minute intervals at 3.5-m altitude, and air temperature, relative humidity, and surface and subsurface temperature and salinity at 10-minute intervals at 3-m altitude. Beginning in May 2005, KEO buoy monitored upper ocean currents at 5-, 15- and 35-m depth, although unfortunately, the 5-m depth current meter failed after less than one month. Details of all sensor specifications and sampling strategies can be found on the KEO webpage: http://www.pmel.noaa.gov/keo/.

[8] Latent heat flux (LHF) and sensible heat flux (SHF) were computed from the high-resolution (10 minute) SST and surface meteorological measurements using the Coupled Ocean-Atmosphere Response Experiment (COARE) bulk algorithm (Version 3.0) [*Fairall et al.*, 2003]. Height correction is applied to bulk parameters observed by KEO buoy. The algorithm's optional warm layer and cool skin temperature corrections were applied to the bulk SST for computation of the fluxes. The algorithm requires winds to be referenced to the surface currents. Because the KEO mooring current meter records are significantly shorter than the study period, following *Cronin et al.* [2006a], we referenced the winds to surface currents using the satellite-derived 15-m current data from the Ocean Surface Current Analyses-Real Time (OSCAR). OSCAR currents are a combination of Ekman and geostrophic currents based on QuikSCAT winds, and TOPEX/Poseidon sea level height measurements [*Bonjean and Lagerloef*, 2002]. The average difference and RMS difference with the KEO 15-m currents were 0.10 m/s and 0.27 m/s, respectively. Because the shear measured between 15 m and the short 5-m record averaged 0.02 m s^{-1} and had an RMS of 0.04 m s^{-1}, we can consider the 15-m current speeds to be surface currents.

[9] Net solar radiation (SWR) was computed by reducing the measured downward solar radiation (DSWR) by a factor of $(a - 1)$, where a, the albedo at the ocean surface, is set as International Satellite Cloud Climatology Project (ISCCP) climatological monthly mean values (http://isccp.giss.nasa.gov/projects/browse_fc.html). The albedo varies from 0.06 in summer to more than 0.1 in winter. Upward longwave radiation was estimated from the fourth power of the sea

Table 1. Results of Error Analysis for Measurement Errors[a]

		W	Ts	Ta	RH	All	All (daily mean)
Assumed Error	RMS	±0.135 m/s	±0.018°C	±0.2°C	±2.7%	-	-
	Random	±0.135 m/s	±0.0153°C	±0.198°C	±2.49%	-	-
	Bias	0 m/s	0.0095°C	0.025°C	1.04%	-	-
LHF W m^{-2}	Random	2.7	0.6	5.9	13.9	15.4	2.3
	Bias	0	0.3	−0.7	−5.2	−5.5	−5.5
SHF W m^{-2}	Random	0.6	0.2	2.7	0	2.8	0.3
	Bias	0	0.1	−0.3	0	−0.2	−0.2

[a]A positive bias between the postcalibration and precalibration indicates that the value based upon the precalibration only may be biased low.

surface temperature (T_s) in units Kelvin, scaled by Stefan-Boltzman constant (σ) and the emissivity at the ocean surface (ε). Following *Konda et al.* [1994], we use an emissivity of 0.984. Net longwave radiation (LWR) was computed as the difference between the estimated upward longwave radiation (ULWR) and the measured downward longwave radiation (DLWR), reduced by the emissivity at the ocean surface. Our sign convention for vertical heat fluxes is that a positive value represents heat loss by the ocean and gained by the atmosphere. Thus the total heat flux (THF) out of the ocean can be represented as

$$\mathrm{THF} = (a-1)\mathrm{DSWR} + \varepsilon\left(\sigma \mathrm{T_s^4} - \mathrm{DLWR}\right) + \mathrm{LHF} + \mathrm{SHF}, \quad (1)$$

where the first term on the RHS is the net solar radiation out of the surface (SWR), the second term is the net longwave radiation out of the surface (LWR), and LHF and SHF are the latent and sensible heat losses.

[10] NRA1 and 2 provide all relevant heat flux components and bulk physical variables. However, the various outputs are not uniformly reliable. The reliability is indicated by a classification flag from A to D. For example, flag "A" means that the analysis is based strongly on observed data, while flag "C" means that the analysis is based on the model alone. All surface heat fluxes analyzed in this study are flagged as C. On the other hand, most physical (meteorological) variables used for estimation of turbulent heat fluxes, such as wind speeds, specific humidity, and air temperature are flagged as A and B [*Kalnay et al.*, 1996]. It should be noted that NRA fluxes are provided as 6-hour average data, while NRA meteorological variables are 6-hour interval data (http://www.cdc.noaa.gov/cdc/data.ncep.reanalysis.surface-flux.html). In particular, the 6-hour flux averages are for the 6 hours following the reference time, while the NRA meteorological variables are forecasted snapshots, valid 6 hours after the reference time. Also it should be noted that the time interval of the original data used for estimation of 6-hour average fluxes is 30 minutes. Spatial resolution for those products is 2.5° × 2.5°. Daily-averages of each flux were computed from the 4-times-per day analyses. NRA data, with T62 spatial resolution (about 210 km), are linearly interpolated to the location of the KEO buoy using the four grid points surrounding the KEO buoy.

[11] Finally, we investigate the KEO measurement accuracy in this section. The results are given in Table 1. We assume the bias and the random error for wind speed, sea surface temperature, atmospheric temperature and relative humidity to be values shown in Table 1. RMS error includes bias and random error (RMS error)^2 = bias^2 + (random error)^2. With the exception of wind, these error estimates are based upon the RMS of the pre- and post-calibration trends of TAO sensors [*Lake et al.*, 2003; *Freitag et al.*, 2005; *Cronin et al.*, 2006a]. Our treatment of the mean trend as a bias will likely overestimate the bias error. The wind speed error is assumed to be the manufacture specified accuracy. Here we assume wind speed error to be random error only, 0.135 m/s. After adding the error value to the observed state variable value, we estimate the impact of each parameter on the error statistics of LHF and SHF. Also we estimate the error statistics for the case of adding the error values for all parameters at the same time. It should be noted that there will be cancellation of errors. As shown in Table 1, measurement error of relative humidity has the largest impact on LHF error, and accounts for most of the total error. The total error for the instantaneous (i.e., 10 minute) LHF is estimated to be ∼16 W m^{-2}. The portion of this error that is random can be reduced through averaging. Thus for daily-averaged LHF, the total error is estimated to be ∼6 W m^{-2}. It should be noted that *Cronin et al.* [2006a] treated the RMS error as a bias and therefore should be compared to the 10-minute (instantaneous) total error estimated here. As expected, the total error is larger in the KEO region than in the tropics owing to the stronger winds. For sensible heat flux, the measurement error of atmospheric temperature is most significant. As shown in Table 1, the total error for SHF is estimated to be 3 W m^{-2}.

3. Comparison of Heat Flux Data

3.1. Shortwave Radiation Flux (SWR)

[12] The daily-mean net shortwave radiation flux observed by the KEO buoy and the differences between the KEO and reanalysis fluxes are shown in Figure 1, with positive values indicating a heat transfer from the ocean to the atmosphere. Shortwave radiation shows remarkable seasonal variability, both in its absolute value and its synoptic variability. The maximum absolute value is about 350 W m^{-2} in summer and 125 W m^{-2} in winter, while the minimum value is about 25 W m^{-2} in both winter and summer. The strong decreases in shortwave radiation, seen intermittently from summer to autumn in 2004, are associated with typhoon passages. As shown in the NRA and KEO difference plot (Figure 1), the reanalyses consistently underestimate the amplitude of these events, reflecting the present capability of typhoon prediction with these numerical weather prediction models.

[13] *Qiu et al.* [2004] found that NRA1 shortwave radiation was larger than observed by a Japan Meteorological

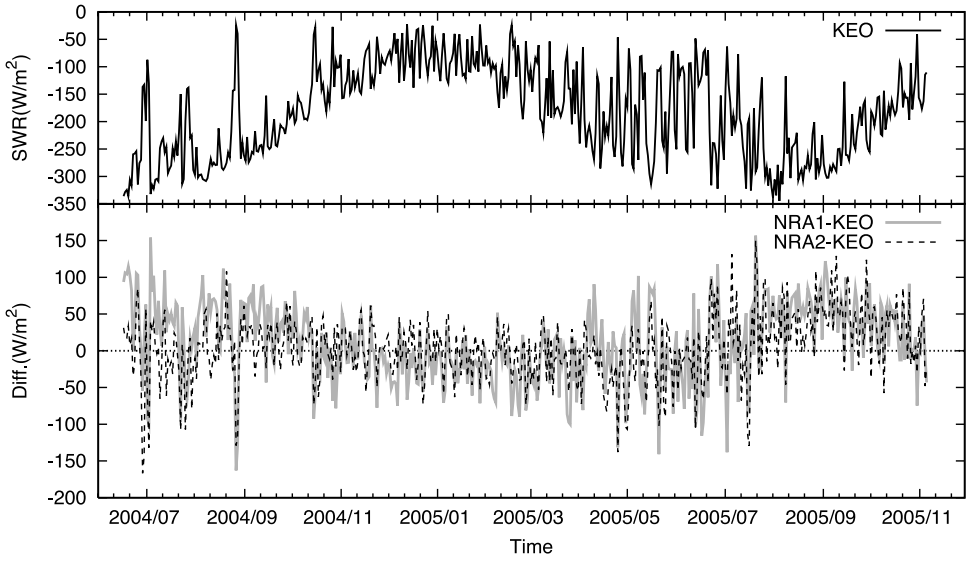

Figure 1. Daily averaged time series of the net solar radiation (SWR) and the differences between KEO and NRA. Positive differences indicate that the amplitude of reanalysis underestimates that of KEO.

Agency buoy at 29°N, 135°E. In contrast, our results show that the NRA shortwave radiation was slightly overestimate from winter to spring, and was underestimated from summer to fall, particularly in 2005. The underestimation in summer leads to overestimation of heat flux from the ocean to the atmosphere. Overall, the NRA1 and NRA2 net shortwave radiation (SWR) RMS error is large, 48 and 38 W m^{-2}, but the bias is relatively small, −1 and 5 W m^{-2}, respectively (Tables 2a and 2b).

[14] Figure 2 shows time variation of the differences of upward shortwave radiation (USWR), and albedo for NRA1, NRA2 and the ISCCP climatological monthly mean values used in this study. The albedo for NRA1 and NRA2 was derived as the ratio of the USWR to the downward shortwave radiation (DSWR) in reanalysis. Interestingly, the albedo is quite different for each product. Although NRA1 albedo is extremely large compared with other products as described in the URL (http://www.cpc.ncep.noaa.gov/products/wesley/reanalysis2/kana/reanl2-1.htm), it reproduces the seasonal variability of the ISCCP albedo. On the other hand, NRA2 albedo has a mean value similar to the ISCCP albedo, but does not reproduce the seasonal variability. Consequently, as shown in Table 3a, differences in the upward SWR between NRA1 and KEO are considerably larger than those between NRA2 and KEO. However, since the NRA1 overestimates both upward and downward SWR by almost the same amount, the net SWR bias for NRA1 is small (Table 2a).

[15] Both NRA1 and NRA2 have considerable RMS error for DSWR (i.e., 40−50 W m^{-2}), due to errors in the total cloud content (TCC). Since the KEO buoy does not directly observe TCC, we only compare TCC of NRA1 and NRA2 in Figure 3. Low-frequency variation of TCC are highlighted using a 30-day running mean. As shown in Figure 3b, in winter NRA2 TCC is significantly larger than NRA1 TCC and contributes to the large difference in the bias for downward SWR between NRA1 and NRA2 shown in Table 3a.

3.2. Longwave Radiation Flux (LWR)

[16] Figure 4 shows time variation of the daily-mean net longwave radiation (LWR) observed by KEO and the differences between KEO and reanalysis fluxes. KEO LWR data are missing in June of 2005 owing to a data gap in DLWR. LWR shows weak seasonal variability, being relatively large in winter and small in summer. In particular, for a short period in July 2005, DLWR was extremely large, causing the net longwave radiation to become negative. Although the shortwave radiation also exhibited a large reduction during this period, the validity of such an extreme event is uncertain. Outside of this event, during summer, the differences between the NRA and KEO LWR are relatively small. On the other hand, during winter, net LWR is overestimated by NRA1 and strongly underestimated by NRA2 in comparison to KEO values. As shown in Table 3b and Figure 5, the errors in net longwave radiation are primarily due to errors in the downward longwave radiation. NRA2 DLWR shows an overestimation in winter of 30−40 W m^{-2}, not found for NRA1. The difference between NRA1 and NRA2 is expected to be related to NRA2 TCC errors which appear to be large during this period (Figure 3). The agreement about the

Table 2a. Statistics for Each Surface Flux Component for NRA1

NRA1	SWR	LWR	LHF	SHF	THF
Correlation	0.80	0.79	0.92	0.93	0.93
RMS Error	48	15	48	20	77
Bias	−1	1	38	9	49

Table 2b. Statistics for Each Surface Flux Component for NRA2

NRA2	SWR	LWR	LHF	SHF	THF
Correlation	0.88	0.78	0.91	0.94	0.94
RMS Error	38	15	62	23	85
Bias	5	−6	60	7	56

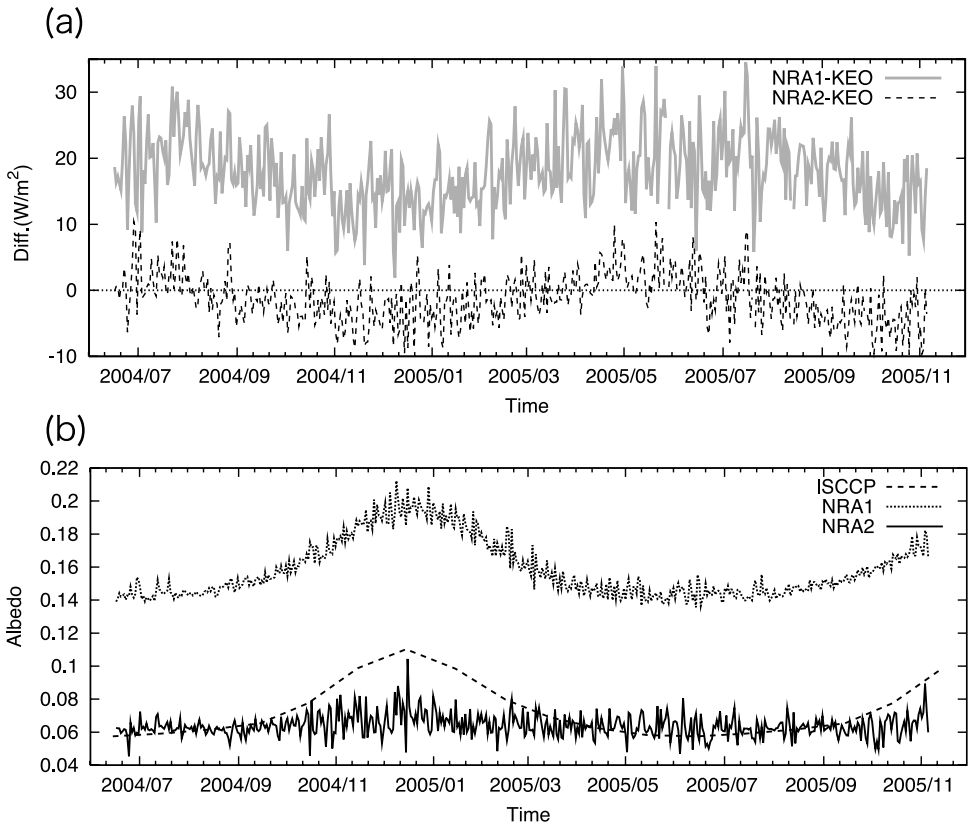

Figure 2. (a) Daily averaged time series of the differences between KEO and NRA. (b) Time variation of albedo.

upward longwave radiation (ULWR) in Table 3b indicates relative agreement in SST.

3.3. Turbulent Heat Fluxes

[17] Time variation of KEO turbulent heat flux is shown in Figure 6. Since we include warm layer and cool skin effects in the estimation of LHF and SHF, and these skin temperature corrections require downward LWR, LHF and SHF are not estimated in June of 2005. Both latent and sensible heat fluxes have extremely large seasonal variations, with large fluxes in winter and small fluxes in summer, as expected. LHF is nearly always larger than SHF and reached more than 400 W m^{-2} in winter. SHF however is not insignificant. In winter, SHF is sometimes more than 100 W m^{-2}.

[18] Both reanalyses overestimated latent heat flux in comparison to KEO, with the overestimation being larger for NRA2 than for NRA1 (Tables 2a and 2b and Figure 6). The LHF bias is 39 W m^{-2} for NRA1 and 61 W m^{-2} for NRA2, respectively. The RMS error is also larger for NRA2 than for NRA1. Both reanalyses however show several large spike differences, 200−300 W m^{-2}, in comparison to KEO LHF during summer and autumn, related to typhoon passages.

[19] There are various possible causes for the difference between KEO and NRA heat fluxes. One cited cause is the use of different flux algorithms for estimating the turbulent heat fluxes. For example, *Brunke and Zeng* [2002] compared eight bulk algorithms and showed significant differences in estimated fluxes due to various differences in the algorithms. To test this hypothesis, we calculated turbulent heat fluxes from NRA meteorological variables using the same bulk algorithm used for computing the KEO turbulent heat fluxes, i.e., the COARE3.0 bulk algorithm. We will refer to the resulting fluxes by COARE3.0 as NRA1C or NRA2C.

[20] Comparing the scatterplots between KEO and NRA1C LHF (Figure 7a) and KEO and NRA1 LHF (Figure 7b), it is clear that using COARE3.0 reduces LHF and the NRA biases (Table 4a), although the reduction in the NRA1C appears to be too great for LHF values above 200 W m^{-2}. Comparing Table 4a with Tables 2a and 2b, we see that the NRA1 LHF RMS error is not largely reduced, while the NRA2 RMS error has a large reduction (from 62 W m^{-2} to 43 W m^{-2}). For SHF, NRAC shows a reduction in bias and RMS error (Tables 2a, 2b,

Table 3a. Comparison Results Between NRA1, and NRA2, and KEO, for Upward Shortwave Radiation and Downward Shortwave Radiation[a]

	USWR, W m^{-2}		DSWR, W m^{-2}	
	NRA1	NRA2	NRA1	NRA2
Correlation	0.65	0.73	0.80	0.88
RMS Error	6	4	52	41
Bias	18	−1	17	4

[a]Upward shortwave radiation, USWR; downward shortwave radiation, DSWR.

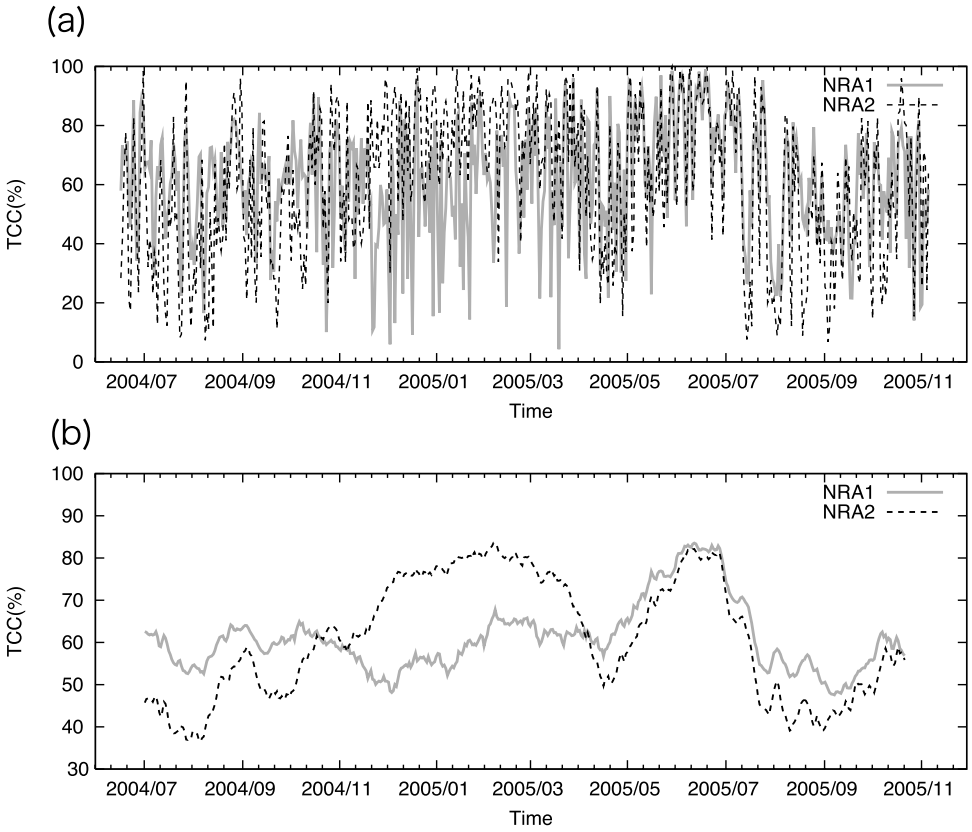

Figure 3. Time series of total cloud content by NRA1 and NRA2. (a) Daily mean data. (b) Low-frequency data.

4a, and 4b). Comparison between the NRA and NRAC fluxes is shown in Figure 7c and Table 4b. Although the correlation coefficients are high, the average difference between NRA1 and NRA1C is large and the LHF appears to be quite sensitive to differences in the bulk algorithm. Which algorithm produces a more accurate LHF and SHF is not determined from this analysis and would require comparisons with direct observations, similar to the analysis of *Fairall et al.* [2003] for the COARE v3 bulk algorithm. Because the COARE v3.0 bulk algorithm is based on more than 5000 direct covariance fluxes collected over the global oceans, we assume that it is the more

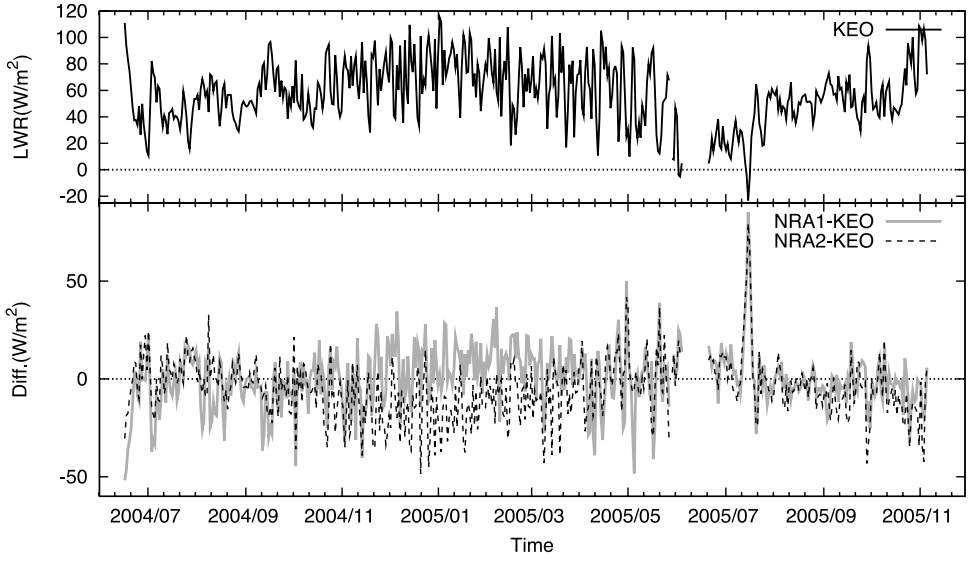

Figure 4. Same as Figure 1, except for the net longwave radiation (LWR).

Table 3b. Comparison Results Between NRA1 and NRA2, and KEO, for Upward Longwave Radiation and Downward Longwave Radiation[a]

	ULWR, W m^{-2}		DLWR, W m^{-2}	
	NRA1	NRA2	NRA1	NRA2
Correlation	0.99	0.99	0.91	0.90
RMS Error	3	4	15	16
Bias	2	2	1	8

[a]Upward longwave radiation, ULWR; downward longwave radiation, DLWR.

accurate bulk algorithm as shown by *Brunke et al.* [2003]. It should be noted, however, that the differences between NRA and NRAC LHF is also partially due to the different meteorological variables used in the estimations. As mentioned earlier, the NRAC LHF is an instantaneous value while NRA LHF is an average value. The results shown here are consistent with the improvement found when the COARE2.6 algorithm was applied to NRA meteorological variables in the Atlantic [*Sun et al.*, 2003] and when the COARE3.0 algorithm was applied to NRA meteorological variables in the tropical Pacific [*Jiang et al.*, 2005]. We conclude that the overestimation of NRA LHF is due largely to the bulk algorithm and is a general feature of the NRA latent heat flux.

[21] In order to identify further causes for the discrepancies in fluxes, we compare meteorological variables observed by KEO with reanalysis. All meteorological data of both reanalyses and KEO sensor were adjusted to a common height using the COARE algorithm. Because the meteorological variable in the reanalysis is not an average value but rather an instantaneous value every 6 hours, we resample KEO data every 6 hours for comparison with the reanalyses' meteorological values.

[22] Figure 8 shows the time variation of each meteorological variable and the difference from KEO data. Since the SST and air temperature variations are quite similar to that of saturated specific humidity (Qs) and specific humidity (Qa), respectively, the temperature comparisons are not shown here. As expected, there exists significant seasonal variability in all variables. While wind speeds are large in winter and small in summer, other variables are vice versa. It should be noted that winds are considerably weaker in summer of 2005 than 2004. *Kako and Kubota* [2007] point out that the increase of heat transfer from the atmosphere to the ocean related to the weak winds contribute to the shallow ocean mixed layer in winter of 2005–2006.

[23] As shown in Figure 8a, in comparison to the KEO, NRA1 underestimate wind speeds and NRA2, particularly during winter, overestimate wind speeds. It is interesting that NRA1 overestimates turbulent heat fluxes compared with KEO fluxes in spite of the underestimation of wind speeds (Table 2a). As discussed earlier, this overestimation could be significantly reduced by using the COARE bulk algorithm with the reanalysis meteorological variables. Therefore we surmise that the differences in the algorithm have a larger impact on the flux comparison than the differences in the wind. This will be verify later in this section.

[24] Both Qs and Qa tend to follow temperature, being large in late summer and small in late winter. NRA1 and NRA2 both overestimate in winter and underestimate in summer air and saturated surface specific humidity. Apparently, in this region, NRA1 and NRA2 moisture fields are quite similar. *Bond and Cronin* [2008] show that during the cool season, prevailing winds at KEO are northerly and are of continental origin, while during the warm season, prevailing winds at KEO are southerly and are of marine origin. The discrepancies in Qa thus could be due to improper boundary layer effects associated with the prevailing winds. Although the differences of saturated specific humidity (Qs) between reanalysis and KEO buoy data are smaller than that of air specific humidity (Qa), the differences of Qs are not negligible. It is interesting that all variables show large differences associated with the Typhoon passages during summer and autumn.

[25] It is difficult to accurately evaluate the contribution of each meteorological variable to the flux error because the bulk formula is nonlinear. Therefore, following *Jiang et al.* [2005] and *Tomita and Kubota* [2006], we use daily-averaged meteorological variables from the KEO buoy, systematically substituting one component parameter with that from NRA1 and NRA2 (these data sets are hereafter referred to as substitute data sets). The three substitute data sets are listed in Tables 5a and 5b and the fluxes computed from the daily-mean KEO meteorological variables are the reference time series. Figure 9 shows the scatterplots of the relation between KEO reference LHF and each substitute data set for NRA1.

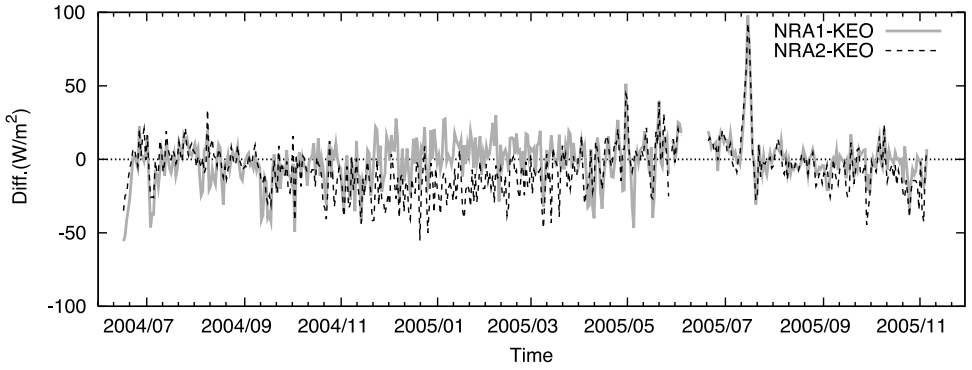

Figure 5. Time variation of the differences of downward longwave radiation (DLWR) between NRA and KEO.

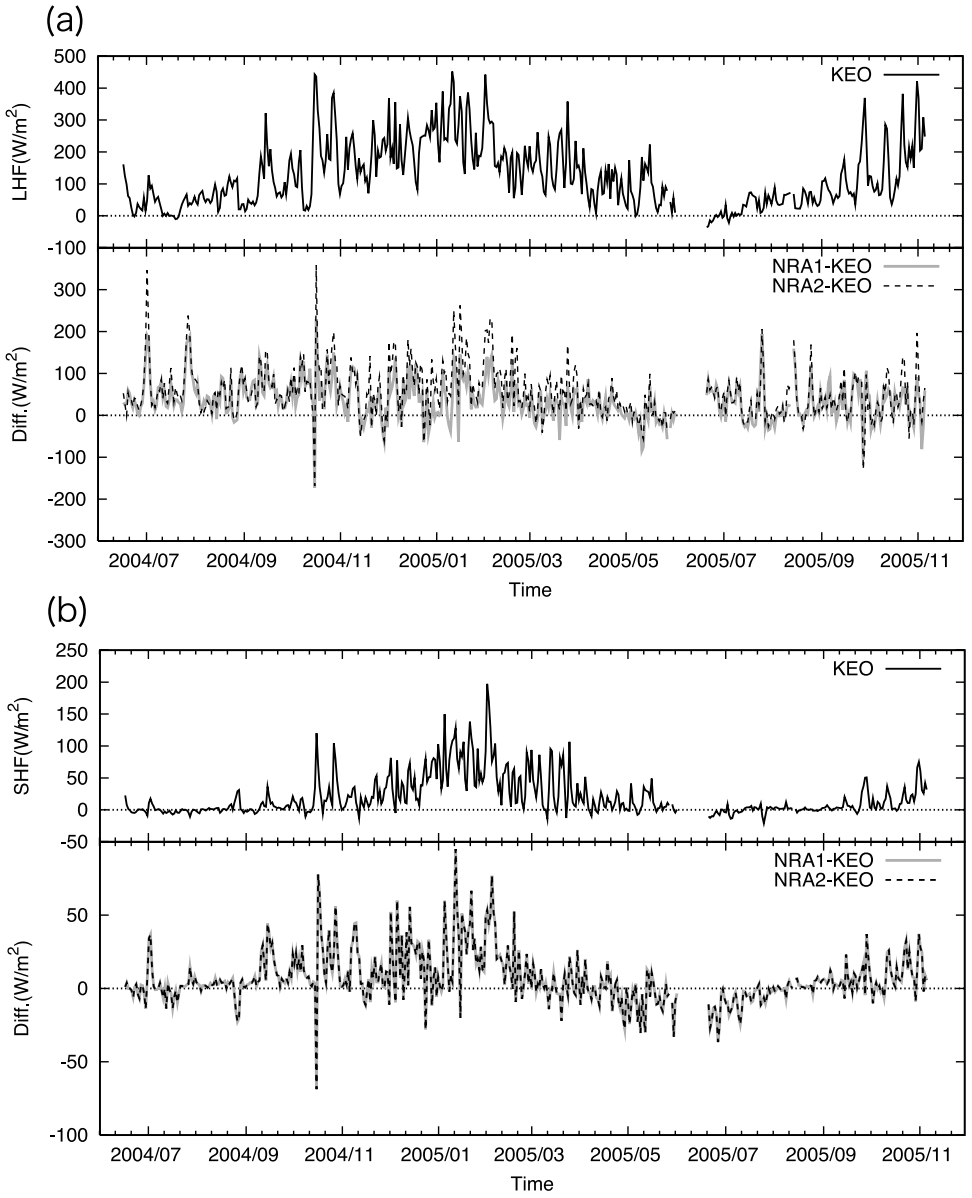

Figure 6. Same as Figure 1, except for (a) latent heat flux (LHF) and (b) sensible heat flux (SHF).

[26] As shown in Tables 5a and 5b and Figure 10, of all the variables, Qa contributes the largest error to the turbulent heat flux, consistent with the results found by *Sun et al.* [2003], *Jiang et al.* [2005], and *Tomita and Kubota* [2006]. For NRA1, errors in Qa contribute 42 W m^{-2} to the RMS error in LHF. Owing to the seasonal errors in Qa, NRA1 Qa overestimates LHF in the lower flux regime and underestimates LHF in the higher flux regime as shown in Figure 9. Although Qa contributes the most to the bias in the turbulent heat flux, it is small compared with the bias caused by the algorithm errors as shown earlier.

[27] The error of NRA LHF also depends to a lesser extent upon errors in wind speed and sea surface temperature. NRA1 wind speeds contribute to the LHF scatter in the higher flux regime. The overestimation due to NRA2 wind speeds is extremely large for LHF in excess of 200 W m^{-2} (not shown here). Alternatively, the buoy wind speed corrected to 10 m might be underestimated during high-wind events owing to the influence of waves on the surface wind profile [*Large et al.*, 1995]. Further work is necessary to understand and improve the accuracy of wind stress and flux calculations in high-wind, high-wave regimes.

[28] The biases due to Qs and WS, although smaller than that due to Qa, are still relatively large, particularly for NRA2 (Tables 5a and 5b). The original temporal resolution of SST used in NRA is weekly and quite low, relative to other newly available global SST data sets, for example, The Center for Atmospheric and Oceanic Studies (CAOS) SST and the Microwave Optimum Interpolation (MWOI) SST [*Iwasaki et al.*, 2008]. CAOS is provided by Tohoku University and MWOI is provided by Remote Sensing Systems (RSS). Therefore, to evaluate the sensitivity of latent heat flux to the assimilated SST field, we estimated LHF and SHF by using Microwave Optimum Interpolation (MWOI) SST instead of NRA1 SST. As shown in Figure 10, the resulting LHF compares much more favorably with the KEO LHF.

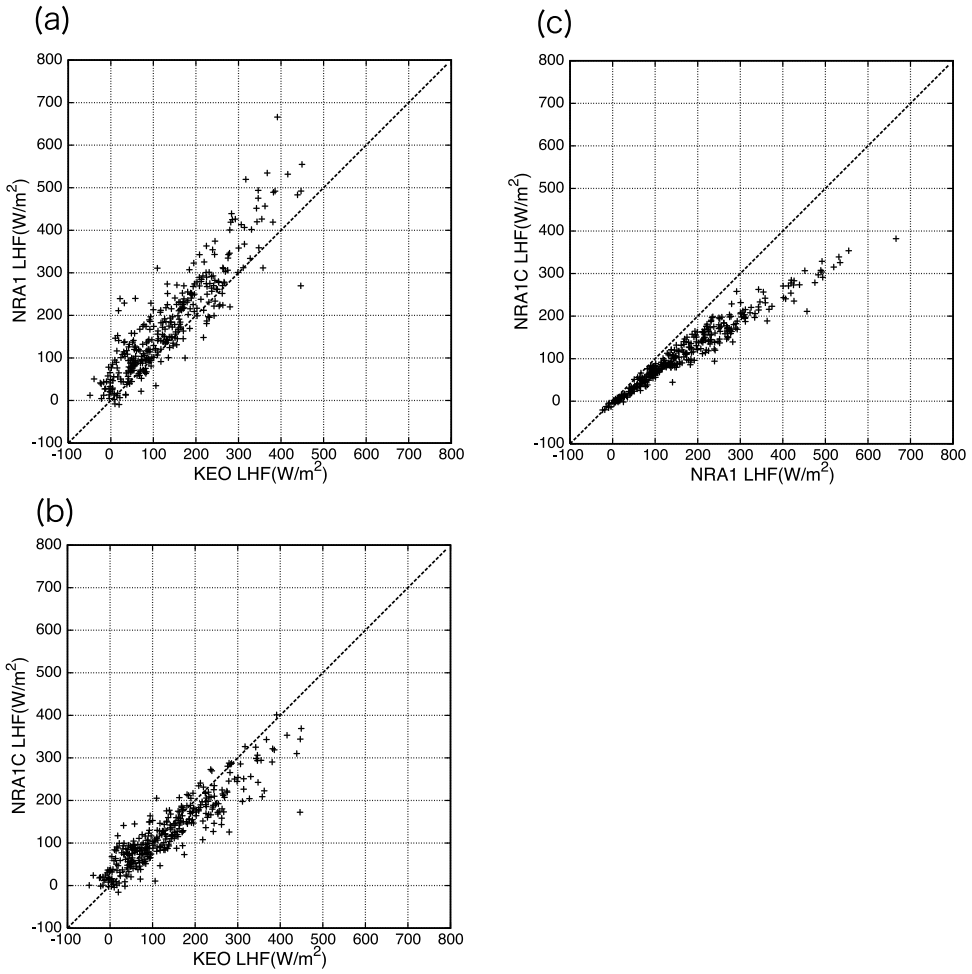

Figure 7. Scatterplots of latent heat flux (LHF) estimated by using meteorological variables. (a) KEO-NRA1, (b) KEO-NRA1C, and (c) NRA1-NRA1C.

This suggests that both reanalyses could be improved by assimilating better SST data.

3.4. Total Heat Flux

[29] Figure 11 shows time variation of total heat flux observed by KEO buoy and the difference between KEO and reanalysis total heat flux. Heat transfer from the ocean to the atmosphere occurs roughly from October to May. Clearly a huge amount of heat energy is released from the ocean to the atmosphere. In particular, the heat transfer reaches to more than 500 W m^{-2} in winter, while the heat gain in summer is at most 200 W m^{-2}. The differences in the total heat flux were relatively large throughout the record, except during spring 2005, when the net surface heat flux was also small. The large differences in winter are due to the large differences of LHF and SHF shown in Figures 6 and 7, while those in summer are due to the large differences in SWR shown in Figure 1, rather than LHF and SHF. As shown in Tables 2a and 2b, the bias of THF strongly depends on that of LHF, while the RMS error of THF is related to both SWR and LHF. Recently, *Kako and Kubota* [2007] pointed out the importance of preconditioning for the formation of ocean mixed layer in winter in the Kuroshio/Oyashio Extension region. Therefore it is crucial to obtain accurate heat transfer not only for winter but also in summer to understand the formation mechanism of ocean mixed layer and Subtropical Mode Water.

[30] Since the differences between KEO and reanalysis THF are mostly positive, both of the reanalyses overesti-

Table 4a. Statistics for Turbulent Heat Flux Component for KEO-NRA1C and KEO-NRA2C

	Latent Heat Flux, W m^{-2}		Sensible Heat Flux, W m^{-2}	
	KEO-NRA1C	KEO-NRA2C	KEO-NRA1C	KEO-NRA2C
Correlation	0.91	0.91	0.92	0.93
RMS Error	43	43	13	15
Bias	−11	13	−3	−3

Table 4b. Statistics for Turbulent Heat Flux Component for NRA1-NRA1C and NRA2-NRA2C

	Latent Heat Flux, W m^{-2}		Sensible Heat Flux, W m^{-2}	
	NRA1-NRA1C	NRA2-NRA2C	NRA1-NRA1C	NRA2-NRA2C
Correlation	0.97	0.98	0.98	0.99
RMS Difference	46	44	15	14
Average Difference	54	50	8	6

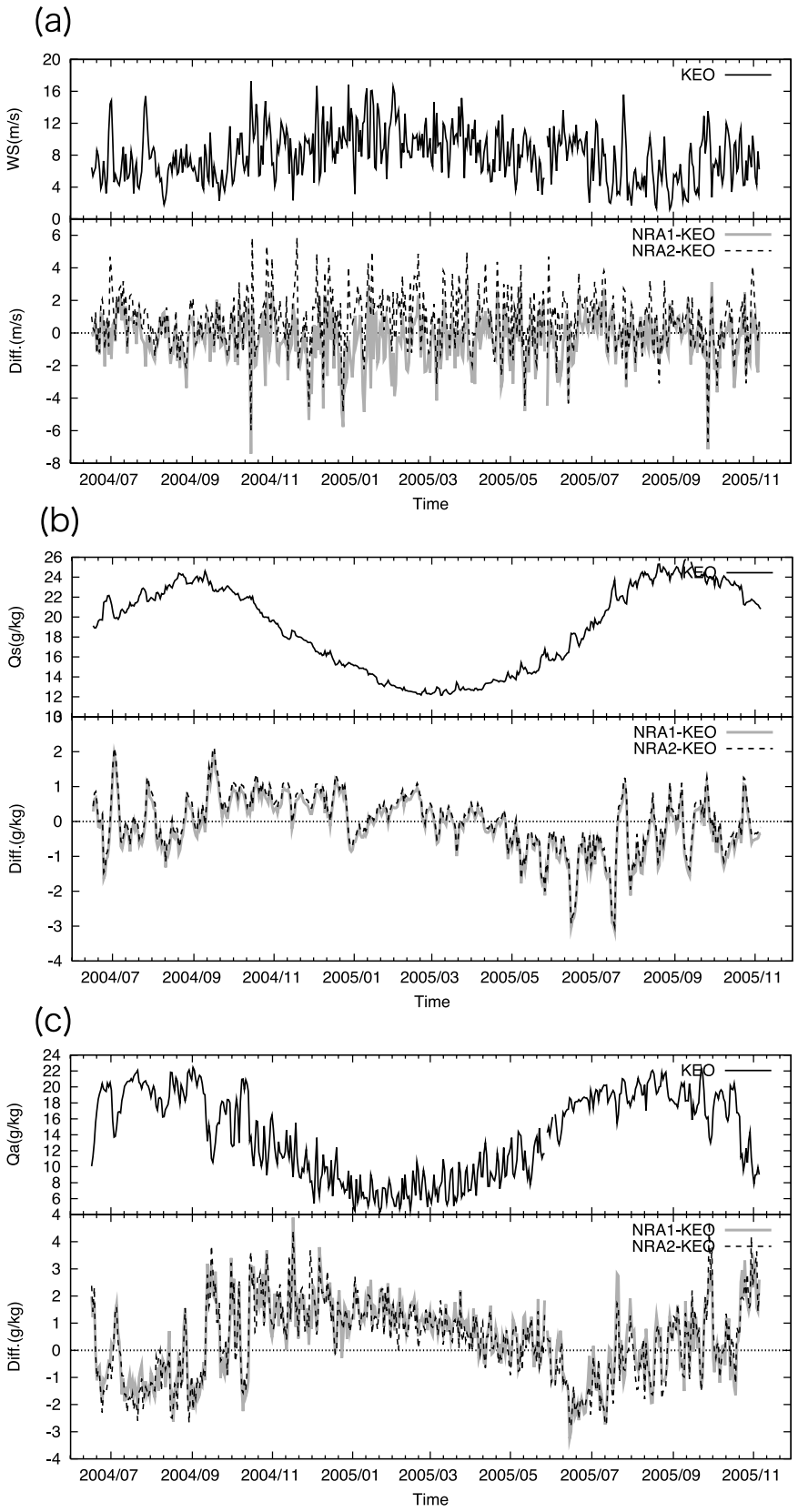

Figure 8. Same as Figure 1, except for (a) wind speed, (b) saturated specific humidity, and (c) specific humidity.

Table 5a. Substituted Data Sets of NRA1 (NRA2) LHF and the Statistics Between KEO Buoy and Each Substituted Data Set for Latent Heat Flux[a]

Data Set	Wind Speed	Sea surface Temperature	Specific Humidity	Correlation	RMS Error	Bias
Substitute 1	NRA1(NRA2)	KEO	KEO	0.96(0.96)	31(38)	−5(18)
Substitute 2	KEO	NRA1(NRA2)	KEO	0.98(0.98)	23(24)	9(14)
Substitute 3	KEO	KEO	NRA1 (NRA2)	0.95(0.95)	41(40)	−24(−24)

[a]Units are W m^{-2}, except correlation.

mate the heat transfer from the ocean to the atmosphere. If reanalysis heat flux is used for driving a numerical ocean general circulation model, the resulting ocean would be too cool, unless other processes such as advection or mixing had compensating errors. This is a serious problem for climate research because of the unrealistic dynamical balance. Of the two reanalyses, NRA1 appears to be slightly better than NRA2, both in terms of the RMS error and the bias (Tables 2a and 2b). As discussed earlier, the large overestimation of LHF by NRA2 compared with NRA1 is due to the larger NRA2 wind speeds shown in Table 5a.

4. Conclusions and Discussions

[31] In this study we have compared the NRA surface heat flux with heat flux from the new OceanSITES time series reference site surface buoy, KEO, in the Kuroshio Extension recirculation gyre. KEO is operated by NOAA Pacific Marine Environmental Laboratory and is based upon TAO buoy technology modified for the harsh conditions of this region. However, unlike buoys from the TAO/Triangle Trans-Ocean Buoy Network (TRITON) array, data from KEO have not been assimilated into reanalysis products. *Tomita and Kubota* [2006] point out that the ERA40 distribution of specific humidity values strongly depends upon the location of the TAO/TRITON buoys. Therefore assessment based upon these nonindependent data will underestimate the true biases and errors in the reanalysis. The KEO buoy, however, provides independent data for assessing NRA1 and NRA2 surface heat fluxes.

[32] Shore-based studies and comparisons with ship-based measurements indicate that the TAO buoys can measure turbulent heat fluxes to within 10 W m^{-2} and total surface heat fluxes to within 10 W m^{-2} if averaged over several days [*Payne et al.*, 2002; *Cronin et al.*, 2006a]. On the other hand, the present study indicates that KEO buoys can measure LHF to within 15 W m^{-2}. The difference might be related to the large amplitude and the large variability of LHF in the Kuroshio Extension region compared with tropical region. Although the measurement error about relative humidity largely contributes to the total measurement error, more than 90%, the large amplitude and the large variability of LHF are mainly caused by those of wind speeds in this region because LHF is proportional to the product of wind speed and humidity difference in a bulk formula.

[33] The overestimation by NRA1 flux has been pointed out by *Moore and Renfrew* [2002] for western boundary regions, by *Josey* [2001] for the subduction region of the Northeast Atlantic, by *Jiang et al.* [2005] for the tropical Pacific, by Cronin et al. [2006a] for the far-eastern tropical Pacific and by *Tomita and Kubota* [2006] for the tropical Pacific and around Japan. The values obtained in this study are considerably larger than those obtained by previous studies. The results suggest that the differences are likely due in part to the buoy location. Because a huge surface heat flux is transferred from the ocean to the atmosphere in the Kuroshio and Kuroshio Extension region, it is perhaps not surprising that the bias and RMS error are large compared with other regions. The KEO buoy is clearly a critical site for monitoring and understanding the global climate system. It should also be pointed out that the large bias and RMS error of NRA flux might be due to the fact that NRA flux are completely independent of the KEO buoy data. Although reanalyses can be improved by assimilating large networks of data, it is important to maintain independent in situ surface flux data as well for validation purposes. The RMS errors and bias for total heat flux are quite large, about 80 W m^{-2} and 50 W m^{-2}, respectively. The large bias is related to LHF, while the large RMS error is related to both LHF and SWR.

[34] The accuracy of the KEO measurements was also assessed by adding measurement errors to observed state variables. After adding the error value to the observed state variable value, we estimate the impact of each parameter on the error statistics of LHF and SHF. The measurement errors of LHF and SHF are likely to be an overestimation because of stronger winds and large variability of state variables presumably. However, the measurement errors are considerably smaller than the differences of turbulent heat fluxes between KEO and reanalysis. Therefore it is concluded that in situ measurements are important as ground-truth measurements.

[35] We investigated two possible causes of errors for turbulent heat fluxes: the bulk algorithm and the meteorological variables. The bulk algorithm has substantial influence on the bias, while the errors in the state variables mainly affect the RMS errors. If we use COARE 3.0

Table 5b. Substituted Data Sets of NRA1 (NRA2) LHF and the Statistics Between KEO Buoy and Each Substituted Data Set for Sensible Heat Flux[a]

Data Set	Wind Speed	Sea surface Temperature	Air Temperature	Correlation	RMS Error	Bias
Substitute 1	NRA1 (NRA2)	KEO	KEO	0.98(0.98)	8(9)	−2(3)
Substitute 2	KEO	NRA1 (NRA2)	KEO	0.98(0.98)	8(9)	2(4)
Substitute 3	KEO	KEO	NRA1(NRA2)	0.96(0.96)	11(11)	−2(−8)

[a]Units are W m^{-2}, except correlation.

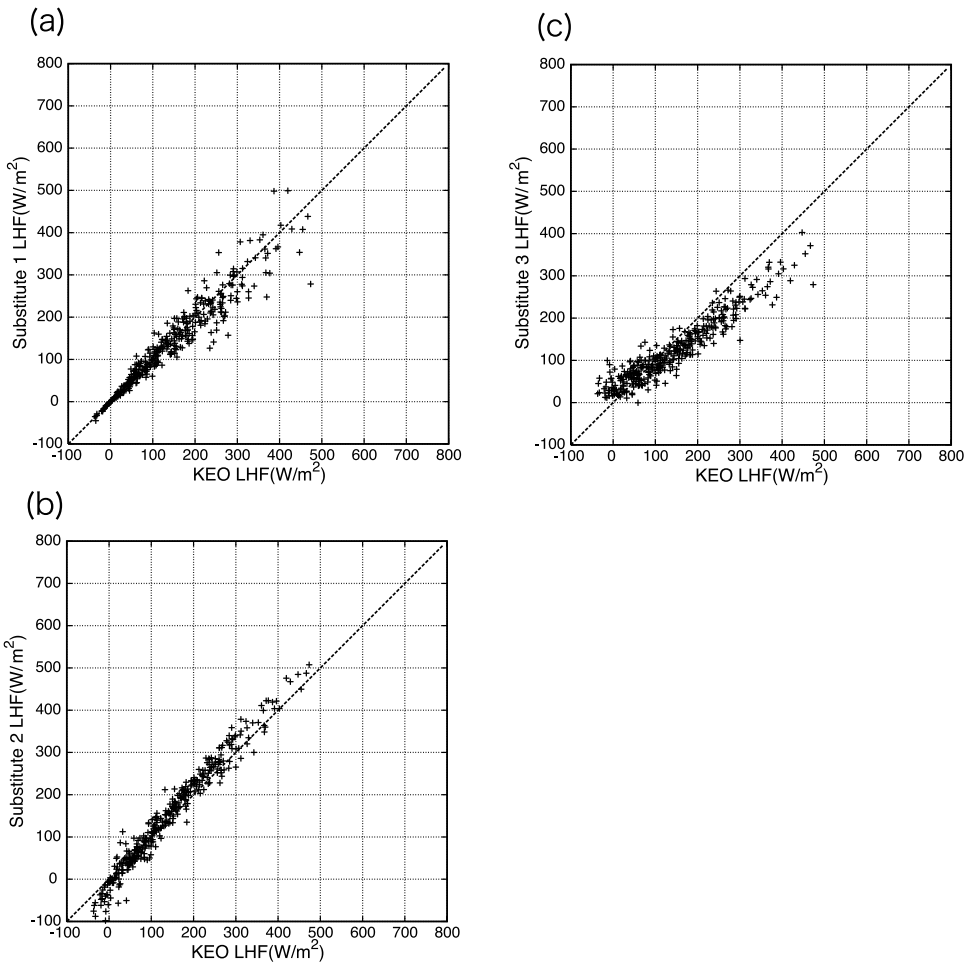

Figure 9. Same as Figure 7, except between KEO latent heat flux and (a) substitute 1, (b) substitute 2, and (c) substitute 3.

algorithm, the bias decreased by about 50 W m^{-2}, with little change in the RMS error. A bias of 50 W m^{-2} over the course of 2 months, corresponds to a temperature bias of 1.2°C for a 50-m-thick layer. For both NRA1 and NRA2 LHF, a specific humidity error is most critical for the RMS error and also contributes to the bias. Since the NRA humidity tended to be too low during the warm season when prevailing winds at KEO were southerly and of marine origin, and tended to be too high during the cool season when prevailing winds at KEO were northerly and of continental origin [*Bond and Cronin*, 2008], the NRA humidity might be improved through better numerical representation of boundary layer processes associated with the prevailing winds. For NRA2 LHF, wind speed discrepancies also contribute to large RMS difference and bias. During high-wind events, large waves can develop that may

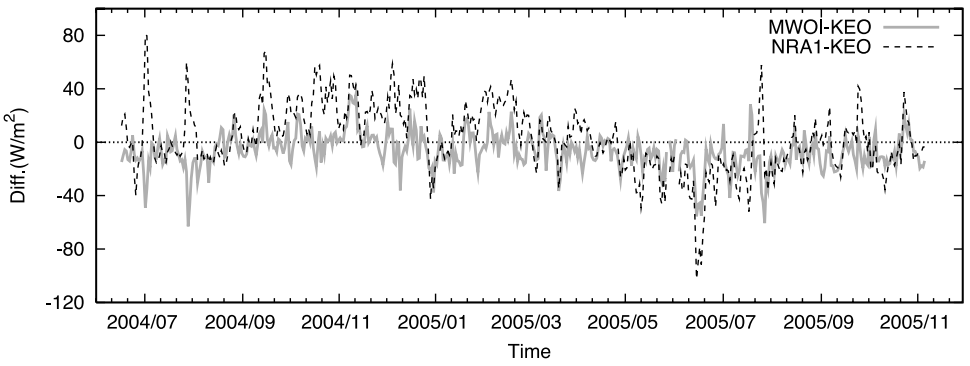

Figure 10. Time variation of the differences between KEO and NRA1 latent heat flux, and KEO and latent heat flux (LHF) estimated using MWOI sea surface temperature (SST).

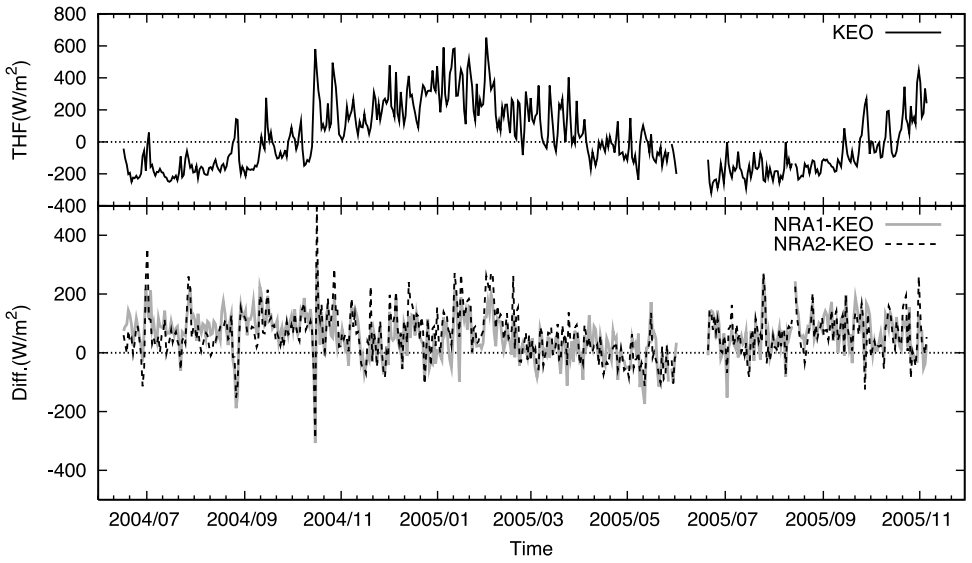

Figure 11. Same as Figure 1, except total heat flux.

distort the wind profile [*Large et al.*, 1995]. If this effect is not accounted for, buoy winds corrected to 10 m height could be biased low. Further work is necessary to understand and improve the accuracy of wind stress and heat flux calculations in high-wind, high-wave regimes. For both NRA1 and NRA2, the turbulent heat fluxes would be improved through assimilation of microwave SST product.

[36] As *Moore and Renfrew* [2002] pointed out the accuracy of the LHF estimation in Kuroshio and Kuroshio Extension regions could be greatly improved through use of a more appropriate bulk algorithm. Although the COARE bulk algorithm used with the KEO buoy data is based upon more than 5000 direct covariance fluxes collected over the global oceans, more high-quality direct flux measurements from research ships in the Kuroshio Extension region are justified. Finally, we plan to expand this study to include not only other reanalyses, such as ERA40 and the Japanese Reanalysis Project (JRA25) [*Onogi et al.*, 2007], but also satellite products such as J-OFURO in the future.

[37] **Acknowledgments.** This research was partly supported by Japan Aerospace Exploration Agency and the Category 7 of MEXT RR2002 Project for Sustainable Coexistence of Human, Nature and the Earth. The KEO buoy was supported by the NOAA Ocean Climate Observations Program. The authors express their deep gratitude to the Kuroshio Extension System Study (KESS) for providing ship time to deploy and turn around the mooring in June 2004, May 2005, and May 2006, and to H. Ichikawa (JAMSTEC) for rescuing the drifting KEO buoy in November 2006. The authors would also like to thank W. Ebisuzaki for his valuable information about NRA products. PMEL contribution 2934.

References

Bond, N. A., and M. F. Cronin (2008), Regional weather patterns during anomalous air-sea fluxes at the Kuroshio Extension Observatory (KEO), *J. Clim.*, in press.

Bonjean, F., and G. S. E. Lagerloef (2002), Diagnostic model and analysis of the surface currents in the tropical Pacific Ocean, *J. Phys. Oceanogr.*, *32*, 2938–2954.

Brunke, M. A., and X. Zeng (2002), Uncertainties in sea surface turbulent flux algorithms and data sets, *J. Geophys. Res.*, *107*(C10), 3141, doi:10.1029/2001JC000992.

Brunke, M. A., C. W. Fairall, X. Zeng, L. Eymard, and J. A. Curry (2003), Which bulk aerodynamic algorithms are least problematic in coupled ocean surface turbulent fluxes?, *J. Clim.*, *16*, 619–634.

Chou, S. H., E. Nelkin, J. Ardizzone, R. M. Atlas, and C. L. Shie (2003), Surface turbulent heat and momentum fluxes over global oceans based on the Goddard Satellite retrievals, version 2 (GSSTF2), *J. Clim.*, *16*, 3256–3273.

Cronin, M. F., C. W. Fairall, and M. J. McPhaden (2006a), An assessment of buoy-derived and NWP surface heat fluxes in the tropical Pacific, *J. Geophys. Res.*, *111*, C06038, doi:10.1029/2005JC003324.

Cronin, M. F., N. A. Bond, C. W. Fairall, and R. A. Weller (2006b), Surface cloud forcing in the east Pacific stratus deck/cold tongue/ITCZ complex, *J. Clim.*, *19*, 392–409.

da Silva, A., C. C. Young, and S. Levitus (1994), *Atlas of Surface Marine Data 1994*, vol. 1, *Algorithms and Procedures, NOAA Atlas NESDIS 6*, 83 pp., NOAA, Silver Spring, Md.

Fairall, C. W., E. F. Bradley, J. E. Hare, A. A. Grachev, and J. B. Edson (2003), Bulk parameterization of air-sea fluxes: Updates and verification for the COARE algorithm, *J. Clim.*, *16*, 571–591.

Freitag, H. P., T. A. Sawatzky, K. B. Ronnholm, and M. J. McPhaden (2005), Calibration procedures and instrumental accuracy estimates of next generation ATLAS water temperature and pressure measurements, *NOAA Tech. Memo. OAR PMEL-128*, 22 pp., Pac. Mar. Environ. Lab., NOAA, Seattle, Wash.

Iwasaki, S., M. Kubota, and H. Tomita (2008), Inter-comparison and evaluation of global sea surface temperature products, *Int. J. Remote Sens.*, in press.

Jiang, C. L., M. F. Cronin, K. A. Kelly, and L. Thompson (2005), Evaluation of a hybrid satellite- and NWP-based turbulent heat flux product using Tropical Atmosphere-Ocean (TAO) buoys, *J. Geophys. Res.*, *110*, C09007, doi:10.1029/2004JC002824.

Josey, S. A. (2001), A comparison of ECMWF, NCEP-NCAR, and SOC surface heat fluxes with moored buoy measurements in the subduction region of the northeast Atlantic, *J. Clim.*, *14*, 1780–1789.

Kako, S., and M. Kubota (2007), Variability of mixed layer depth in the Kuroshio/Oyashio Extension region: 2005–2006, *Geophys. Res. Lett.*, *34*, L11612, doi:10.1029/2007GL030362.

Kalnay, E. M., et al. (1996), The NCEP/NCAR 40-year reanalysis project, *Bull. Am. Meteorol. Soc.*, *77*, 437–471.

Kanamitsu, M., W. Ebisuzaki, J. Woollen, P. Potter, and M. Fiorion (2000), An overview of NCEP/DOE reanalysis-2, paper represented at Second WCRP International Conference on Reanalysis, World Meteorol. Org., Reading, U.K.

Konda, M., N. Imasato, K. Nishi, and T. Toda (1994), Measurement of the sea surface emissivity, *J. Oceanogr.*, *50*, 17–30.

Kubota, M., N. Iwasaka, S. Kizu, M. Konda, and K. Kutsuwada (2002), Japanese Ocean Flux Data Sets with Use of Remote Sensing Observations (J-OFURO), *J. Oceanogr.*, *58*, 213–225.

Lake, B. J., S. M. Noor, H. P. Freitag, and M. J. McPhaden (2003), Calibration procedures and instrumental accuracy estimates of ATLAS air temperature and relative humidity measurements, *NOAA Tech. Memo. OAR PMEL-123*, 23 pp., Pac. Mar. Environ. Lab., NOAA, Seattle, Wash.

Large, W. G., J. Morzel, and G. B. Crawford (1995), Accounting for surface wave distortion of the marine wind profile in Low-Level Ocean Storms wind measurements, *J. Phys. Oceanogr.*, *25*, 2959–2971.

McPhaden, M. J., et al. (1998), The Tropical Ocean Global Atmosphere (TOGA) observing system: A decade of progress, *J. Geophys. Res.*, *103*, 14,169–14,240.

Moore, G. W. K., and I. A. Renfrew (2002), An assessment of the surface turbulent heat fluxes from the NCEP-NCAR reanalysis over the western boundary currents, *J. Clim.*, *15*, 2020–2037.

Onogi, K., et al. (2007), The JRA-25 reanalysis, *J. Meteorol. Soc. Jpn.*, *85*, 369–432.

Payne, R. E., et al. (2002), A comparison of buoy meteorological systems, *WHOI Tech. Rep. WHOI-2002-10*, 67 pp., Woods Hole Oceanogr. Inst., Woods Hole, Mass.

Qiu, B., S. Chen, and P. Hacker (2004), Synoptic-scale air-sea flux forcing in the western North Pacific: Observations and their impact on SST and the mixed layer, *J. Phys. Oceanogr.*, *34*, 2148–2159.

Sun, B., L. Yu, and R. A. Weller (2003), Comparison of surface meteorology and turbulent heat fluxes over the Atlantic NWP model analyses versus moored buoy observations, *J. Clim.*, *16*, 679–695.

Tomita, H., and M. Kubota (2006), An analysis of the accuracy of Japanese Ocean Flux data sets with Use of Remote Sensing Observations (J-OFURO) satellite-derived latent heat flux using moored buoy data, *J. Geophys. Res.*, *111*, C07007, doi:10.1029/2005JC003013.

M. F. Cronin, Pacific Marine Environmental Laboratory, NOAA, Building 3, 7600 Sand Point Way NE, Seattle, WA 98115, USA. (meghan.f.cronin@noaa.gov)

N. Iwabe and M. Kubota, School of Marine Science and Technology, Tokai University, 3-20-1, Shimizu-Orido, Shizuoka 424-8610, Japan. (iwabe@mercury.oi.u-tokai.ac.jp; kubota@mercury.oi.u-tokai.ac.jp)

H. Tomita, Institute of Observational Research for Global Change, Japan Agency for Marine and Earth Science Technology, 2-15 Natsushima-cho, Yokosuka-city, Kanagawa, 237-0061, Japan. (tomitah@jamstec.go.jp)